



Research article

Multi-b-value diffusion weighted imaging for preoperative evaluation of risk stratification in early-stage endometrial cancer



Qi Zhang^a, Xiaoduo Yu^a, Meng Lin^a, Lizhi Xie^b, Miaomiao Zhang^a, Han Ouyang^{a,*},
Xinming Zhao^{a,*}

^a Department of Radiology, National Cancer Center/National Clinical Research Center for Cancer/Cancer Hospital, Chinese Academy of Medical Sciences and Peking Union Medical College, Beijing, 100021, China

^b GE Healthcare, MR Research China, Beijing, China

ARTICLE INFO

Keywords:

Endometrial cancer
Risk stratification
Multi-b-value diffusion weighted imaging (DWI)
Perfusion
Diffusion

ABSTRACT

Purpose: To investigate the application of multi-b-value DWI parameters for the assessment of risk stratification in early-stage endometrial cancer (EC).

Material and methods: Fifty-three patients with early-stage EC who preoperatively underwent multi-b-value DWI with 13 b values (from 0 to 2000s/mm²) were included in this study. Multi-b-value DWI derived parameters, including apparent diffusion coefficient (ADC), true diffusivity (D), perfusion-related diffusivity (D*) and perfusion fraction (f) were measured independently by two radiologists. In addition, binary logical regression model was used to calculate predicative probability of combined parameters indicating statistical significance in differentiating risk stratification of early-stage endometrial cancer. Receiver operating characteristic analysis was performed for all single and combined parameters.

Results: The ADC and D values were significantly lower in intermedium-risk compared with low-risk ($P = 0.000$ and 0.011), as well as high-risk compared with low-risk of early-stage EC ($P = 0.001$ and 0.013), while f values only showed significant differences between low-risk and intermedium-risk groups ($P = 0.011$). Among the single parameters, the ADC values had the highest area under the ROC curve (AUC) in the identification of the low-risk of early-stage EC (AUC = 0.892). Moreover, the combination of ADC and f value had the best diagnostic performance with the AUC of 0.912, the sensitivity of 81.1% and the specificity of 87.5%.

Conclusion: The multi-b-value DWI parameters provide valuable imaging biomarkers for the assessment of risk stratification in early-stage endometrial cancer. This approach might facilitate the selection of the optimal therapeutic approach and lead to the greater personalization of cancer care.

1. Introduction

Endometrial cancer (EC)¹ is the most common gynecologic malignancy in the developed countries. Its incidence is increasing with age and with the increased prevalence of obesity. In the United States, 61,380 women were diagnosed with EC and 10,920 died from this condition in 2017 [1]. In addition, approx. 80% of patients have been diagnosed with EC at early-stage (stage IA and IB); however, the recurrence rate at this stage varies from 2%–26% [2,3], which is mainly associated with the depth of myometrial invasion, lymphovascular

space invasion (LVSI)², histological grade and type [4,5]. For example, the incidence of lymph node metastases increases from 3% with superficial myometrial invasion to 46% with deep myometrial invasion [6,7]. In clinical practice, the risk stratification of early-stage EC has been developed to precisely guide decision-making with the aim to prevent over- and under-treatment of EC. According to the EMSO³ clinical practice guideline for EC [8], early-stage EC were stratified into three classes of risk determining the management strategy and prognosis: low-risk (endometrioid type; stage IA with grade 1 or grade 2), intermedium-risk (endometrioid type; stage IA with grade 3 or stage IB

* Corresponding authors at: Department of Radiology, National Cancer Center/National Clinical Research Center for Cancer/Cancer Hospital, Chinese Academy of Medical Sciences and Peking Union Medical College, Beijing, 100021, China.

E-mail addresses: hoybj@126.com (H. Ouyang), xinmingzh@sina.com (X. Zhao).

¹ EC: endometrial cancer.

² LVSI: lymphovascular space invasion.

³ EMSO: European Society for Medical Oncology.

with grade 1 or grade 2) and high-risk (stage IB with grade 3 or non-endometrioid type). For patients with low-risk EC, lymphadenectomy (LND)⁴ is not recommended since it may increase complications and further costs of care without any disease-free or overall survival benefits. Nevertheless, since LND may significantly improve the outcomes in patients at intermediate- or high-risk of recurrence [9], it is extremely important to explore an effective method for accurate assessment of the risk stratification in the early-stage EC to ensure that each EC patient benefits from individualized cancer care and to ultimately improve treatment approach and outcomes.

Magnetic resonance (MR) imaging has been widely accepted for the evaluation of the local extend and extrauterine tumor spread of EC owing to its superior contrast resolution and excellent soft tissue differentiation. However, conventional MRI is susceptible to coexisting leiomyomas or adenomyosis, loss of junctional zone and myometrium compression due to large tumor [10]. It has been reported that conventional MRI is still not recommended for surgical staging [11,12] due to the poor-to-moderate pooled sensitivity of 80.7% in detecting high-risk factors including deep myometrial invasion and cervical stromal infiltration. In addition, conventional MRI can only provide qualitative information and it lacks specific parameters regarding tumor microstructure or biological information, which are essential for guiding the therapeutic strategy against the individual tumors. To date, diffusion-weighted imaging (DWI)⁵ has been used as an adjunct to conventional MRI for the assessment of EC in many centers to reflect tumor microstructure based on its sensitivity to water molecular diffusion in the tissue intra- and extracellular space [13]. Decreased movement of water molecules in highly cellular tissue is correlated with high signal intensities in DWI images, which can be quantified by apparent diffusion coefficient (ADC)⁶. Yet, the measurement of the conventional DWI signal decay are based on a monoexponential model, which is relatively simplistic for tumor microstructure and does not maximize useful information potentially extracted from DWI [14]. The ADC value can be affected by the blood microcirculation in capillaries leading to an overestimation of the ADC values. Intravoxel incoherent motion (IVIM)⁷, introduced by Le Bihan et al. [15], is a more advanced MR technique, which has the potential to simultaneously measure tissue diffusion and perfusion via multi-b-value DWI and a biexponential model without any of the exogenous contrast media. Many studies on multi-b-value DWI derived parameters have shown promising results for preoperatively grading, staging or evaluating treatment response in several kinds of cancers such as cervical, rectal, liver and brain cancer [16,17]. Nevertheless, the investigation of multi-b-value DWI in preoperative assessment of endometrial carcinoma is still lacking.

The aim of this study was to explore the utility of multi-b-value DWI derived parameters for the assessment of risk stratification in early-stage EC preoperatively.

2. Material and methods

2.1. Study population

A total of 70 consecutive patients suspected of having EC were enrolled and were scheduled for pelvic MRI (with multi-b-value DWI for the initial assessment of tumor characteristics) before surgery at our hospital between September 2016 and August 2017. The inclusion criteria were the following: 1) patients suspected of having EC at dilatation and curettage surgery; 2) patients who did not receive any tumor related treatments before pelvic MRI examination and surgery. Seventeen patients were excluded: 1) according to the advanced

International Federation of Gynecology and Obstetrics (FIGO)⁸ stage [stage II (n = 6), III (n = 4) and IV (n = 2)]; 2) no tumor was detected by MRI or tumor was too small (n = 4); 3) poor image quality (n = 1). Finally, 53 patients were included in the study.

Our Institutional Review Board approved this prospective study and informed consent was obtained from all patients.

2.2. Conventional MR imaging

All MRI examinations were performed on a 3.0 T MRI system (Discovery MR 750, GE Medical System, Milwaukee WI) by using an eight-element phased coil with patients in the supine position. All patients were instructed to fast and abstain from food for 4 h prior to MRI examination. In addition, patients who had no contraindication received 10 mg raceanisodamine hydrochloride injection intramuscularly before image acquisition to reduce the bowel motion artefacts. Detailed imaging parameters are described in Table 1.

2.3. Multi-b-value DW imaging

Multi-b-value DWI were performed before administration of contrast agent in the axial plane, by using the single shot echo-planar imaging pulse sequence in free-breathing. A parallel imaging with a twofold acceleration factor was used to decrease echo train length. Encoding was performed in three perpendicular directions (x, y and z) with 13 b values with different number of excitations: 0(2), 10(2), 25(2), 50(2), 75(2), 100(1), 150(1), 200(1), 400(1), 800(1), 1000(4), 1500(6), 2000(6) s/mm². The parameters were as follows: repetition time/echo time, 4000/68.8 ms; matrix, 128 × 128; field of view, 38 cm; section thickness/intersection gap, 5/1 mm; number of slices, 24 slices for each b value; bandwidth, 250 kHz; and acquisition time, 6 min.

2.4. Imaging analysis

The obtained diffusion weighted imaging was processed using the prototype software provided by the manufacture (GE Healthcare) to acquire diffusion and perfusion parameters.

2.5. Bi-exponential modeling of multi-b-value DWI

Based on the IVIM theory assuming a “microvascular” and “non-vascular” compartment, the IVIM-derived parameters including D, D* and f values were obtained and fitted to the following nonlinear biexponential decay function:

$$\frac{S}{S_0} = (1 - f)\exp(-b \times D) + f \exp(-b \times D^*)$$

where S is the signal intensity of each non-zero b value, S₀ is the signal intensity of b₀ image (b = 0 s/mm²); D, the slow-moving diffusion coefficient, is the true diffusion coefficient representing pure water molecular diffusion in biologic tissues; D*, the fast-moving diffusion coefficient, is the perfusion-related coefficient reflecting the incoherent movements of microvascular blood within the voxel; and f, the perfusion fraction, showed the volume fraction of random microcirculation over the total incoherent signal in each voxel.

2.6. Monoexponential modeling of multi-b-value DWI

The ADC was acquired by using all b values (0–2000s/mm²) fitted to the following monoexponential equation:

⁸ FIGO: International Federation of Gynecology and Obstetrics.

⁴ LND: lymphadenectomy.

⁵ DWI: diffusion-weighted imaging.

⁶ ADC: apparent diffusion coefficient.

⁷ IVIM: intravoxel incoherent motion.

Table 1
Imaging protocol.

	Axial T1WI	Axial T2WI	Sag T2WI	Axial oblique T2WI	Sag DCE	Coronal DCE	Axial DCE
Sequence	LAVA-Flex	FS FSE	FSE	FSE	3D LAVA-XV	3D LAVA-XV	3D LAVA-XV
TR (ms)	4.2	4899.0	4270.0	5500.0	4.5	3.7	7.9
TE (ms)	1.3	85.0	85.0	102.0	1.3	1.7	4.1
Field of view (mm)	34.0	34.0	30.0	22.0	34.0	42	35.0
Slice thickness/gap	3.0/0	5.0/0.5	4.0/1.0	3.0/0	3.0/0	3.0/0	1.0/0
Average (NEX)	1.0	2.0	2.0	4.0	1.0	2.0	1.0
Acquisition time	23(s)	2.03(min)	2.38(min)	2.40(min)	5.37(min)	31(s)	19(s)

DCE = dynamic contrast enhanced; FS = fat suppression; FSE = fast-recovery fast spin echo; LAVA-Flex = Liver Acquisition with Volume Acceleration; LAVA-XV = liver acquisition with volume acceleration - extended volume; NEX = number of excitations; Sag = sagittal; TR = repetition time; TE = echo time; T1WI = T1-weighted imaging; T2WI = T2-weighted imaging.

$$\frac{S}{S_0} = \exp(-b \times ADC)$$

where S_0 is the signal intensity observed in the absence of a diffusion gradient.

2.7. Regions of interest (ROIs)

All images were transferred to the workstation (Advantage Workstation 4.6; GE Medical System) for quantitative analysis of multi-b-value DWI. Two radiologists (X.Y. with 15 years of experience in genitourinary imaging diagnosis and Q.Z with 5 years of experience in genitourinary imaging diagnosis) who were blinded to each other's results placed the ROIs independently. The two radiologists were only aware of patients' diagnosis of EC, but they did not know about tumor final detailed histopathological information, including FIGO stage, tumor histological grade, histopathological subtype, the depth of myometrial invasion, etc.

The Function tool MADC program was used to process the multi-b-value DWI protocol to obtain the parametric maps. A single representative region of interest (ROI) was manually drawn along the margin of the tumor on the image of b_{1000} , on the section containing the largest tumor cross-section area avoiding the areas of necrosis and hemorrhage with reference to other MR images T2WI or dynamic contrast enhanced (DCE) MRI. All ROIs were directly co-localized on all parametric maps, and the software was used to automatically generate the multi-b-value DWI parameters.

2.8. Histological analysis

Histopathological information was obtained by another radiologist (H.OY with 25 years of experience in genitourinary imaging diagnosis) from the pathology reports in the patients' medical reports. Tumor grade, the depth of myometrial invasion (superficial invasion: confined to the endometrium or inner half of the myometrium; deep invasion: invading the outer half of the myometrium), presence of lymphovascular space invasion (LVSI) and histopathological type were recorded.

2.9. Statistical analysis

Statistical analyses were performed with software (MedCalc Software 15.8 and SPSS version 21.0). Data were shown as mean \pm standard deviation or median and range. Interobserver reliability of these parameters was evaluated by using the intraclass correlation coefficient (ICC). ICC values < 0.40 indicated poor reproducibility; ICC values of $0.40-0.75$ indicated fair to good reproducibility; and ICC > 0.75 indicated excellent reproducibility. Kolmogorov-Smirnov tests were used to check the distribution of the multi-b-value DWI parameters. The Spearman rank correlation test was used to assess the relationship between these parameters with risk stratification in early-

stage EC. The correlation coefficient rho (r) was obtained to compare the degree of correlation as follows: little or no relationship if $0 \leq r < 0.25$, fair if $0.25 \leq r < 0.5$, moderate to good if $0.5 \leq r < 0.75$, and very good to excellent if $0.75 \leq r$. The one-way analysis of variances (ANOVA) with post-hoc analysis or Kruskal-Wallis test was used to compare these parameters in the three risk stratification groups. The statistical significance threshold of this comparative test was set at p-value below 0.05, and at p-value below 0.018(0.05/3) for post hoc tests. Moreover, binary logical regression model was used to calculate predicative probability of combined parameters indicating statistical significance in differentiating risk stratification in early-stage EC.

Receiver operating characteristic curve (ROC) was performed by using MedCalc to obtain the area under the receiver operating characteristic curve (AUC), and the optimal cut-off value, sensitivity and specificity of single and combined multi-b-value DWI parameters were automatically calculated. Next, the comparison of ROC curves was performed to evaluate the diagnostic capacity of those single and combined parameters in the assessment of risk stratification in the early-stage EC preoperatively.

3. Results

3.1. Histological finding

All of the 70 patients underwent surgery at our institution. After excluding 17 patients for previously listed reasons, 53 patients remained for final investigation (Fig. 1). The median interval between pelvic MRI examination and surgeries was 12 days (range, 1–36 days). Clinical and pathological characteristics of the eligible patients are shown in Table 2.

3.2. Interobserver agreement

The interobserver variability of manually drawn ROIs was relatively small for the multi-b-value DWI parameters. The interobserver agreement was highest for ADC (ICC, 0.989; 95% confidence interval [CI], 0.983–0.993) and lowest for D^* (ICC, 0.954; 95% CI, 0.926–0.972). The interobserver agreement for the D and f values was also good and the ICC values were 0.971 (95% CI, 0.953–0.982) and 0.964 (95% CI, 0.942–0.978), respectively. Since the interobserver agreement for the multi-b-value DWI parameters was good, only the first reader results were used for further analysis. The Bland-Altman analysis also showed excellent repeatability between the two researchers (Fig. 2).

3.3. Association of early-stage EC risk stratification with the multi-b-value DWI parameters

Except D^* values ($r = 0.116$, $P = 0.407$), the ADC, D and f values showed a significant inverse correlation with the risk stratification at

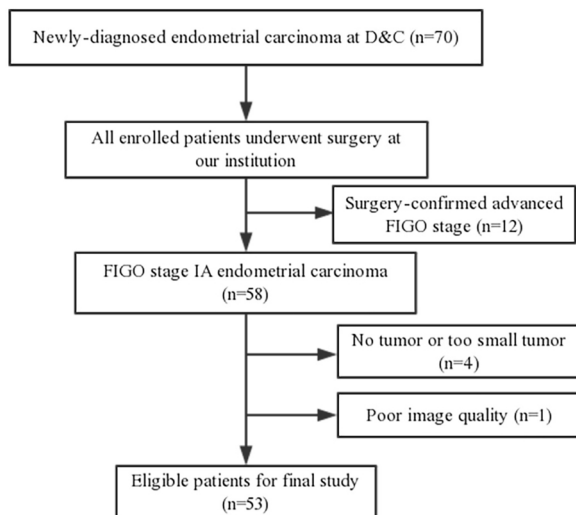


Fig. 1. Flow diagram of study population. D&C: dilatation and curettage surgery; FIGO: International Federation of Gynecology and Obstetrics.

Table 2
Patients age and tumor characteristics.

Variable	Data
Age(mean \pm SD) (years)	53 \pm 9
FIGO stage n (%)	
IA	43(81.1)
IB	10(18.9)
Myometrial invasion n (%)	
Superficial myometrial invasion	43(81.1)
Deep myometrial invasion	10(18.9)
Lymphovascular space invasion n (%)	
Positive	42(79.2)
Negative	11(20.8)
Histologic subtype n (%)	
Endometrioid adenocarcinoma	52(98.1)
Non-endometrioid adenocarcinoma	1(1.9)
Histologic grade n (%)	
Grade 1	14(26.4)
Grade 2	27(50.9)
Grade 3	12(22.7)
Risk stratification (stageI) n (%)	
Low-risk group	37(69.8)
Intermediate-risk group	10(18.9)
High-risk group	6(11.3)

early-stage EC ($r = -0.616$, -0.521 , and -0.385 ; $P = 0.000$, 0.000 and 0.004 , respectively).

The ADC and D values were significantly lower in intermediate-risk compared with low-risk, as well as high-risk compared with low-risk in early-stage EC, while f values only showed significant differences between low-risk and intermediate-risk groups ($P = 0.011$). All these parameters did not show any significant differences between intermediate-risk and high-risk in early-stage EC. After combining the intermediate-risk group with the high-risk group (named as non-low-risk group), the ADC, D and f values of non-low-risk group were statistically significant compared with the low-risk group ($P = 0.000$, 0.000 and 0.010 , respectively) (Table 3; Fig. 3). Two examples are shown in Figs. 4 and 5.

3.4. Diagnostic performance of single and combined multi-b-value DWI parameters for differentiating low-risk from non-low-risk in early-stage EC

According to ROC curves results, AUC was the largest for ADC values (AUC = 0.892; $P < 0.0001$) among those single parameters (AUC for D values: 0.823, $P < 0.001$; AUC for f values: 0.765, $P = 0.001$) in

differentiating low-risk group from non-low-risk group. Based on ROC curves, an ADC higher than $0.830 \times 10^{-3} \text{ mm}^2/\text{s}$ was associated with a low-risk of early-stage EC with the sensitivity of 78.4%, the specificity of 87.5% and the accuracy of 81.1%. The combination of ADC and f values showed the highest AUC 0.912 ($P < 0.0001$) in differentiating low-risk group from non-low-risk group at the optimal cut-off value of 0.701 with the sensitivity of 81.1%, the specificity of 87.5% and the accuracy of 83.0%, followed by the AUC 0.904 for the combination of ADC and D values and the AUC 0.894 for the combination of D and f values (Table 4; Fig. 6).

4. Discussion

Over recent years, novel treatment modalities have created a shift in the medical decision processes for EC [18–20]. Individualized medical care is highly warranted so that each patient with EC can benefit from a personalized and customized treatment approach leading to a progression from broad assessment of tumor anatomic site or morphological characterization to specific evaluation of tumor microenvironment information. In our study, we evaluated the multi-b-value DWI parameters as a diagnostic tool for the assessment of initial risk stratification in early-stage EC. The present study demonstrated excellent interobserver agreement of these parameters, which can be used as a preoperative diagnostic tool for potentially successful clinical implementation.

For early-stage EC, the results of two randomized clinical trials (RCTs) [21,22] showed no therapeutic value of lymphadenectomy. The ESMO-ESGO-ESTRO⁹ consensus conference on EC [23] has suggested that lymphadenectomy is not recommended for patients with low-risk EC (endometrioid type; stage IA with grade1 or grade 2). Theoretically, the higher stratification risk in early-stage EC indicates a more aggressive form of the tumor, which suggests that the tumor microenvironment changes along with the tumor progression including cell proliferation, cellularity count, and microvessel density. Kishimoto et al. [24] have shown a significant inverse relationship between ADC values and tumor cellularity in EC ($r = -0.74$, $P < 0.01$). Jiang et al. [25] have demonstrated that the mean ADC values are negatively correlated with Ki-67 expression ($r = -0.82$, $P < 0.001$), which is an index reflecting the extent of proliferative activity and more aggressive tumors. These findings suggest that the diffusion parameters could be used as a potential tool for the evaluation of risk stratification in early-stage EC. Our preliminary results showed that the diffusion parameters ADC and D values had significantly adverse association with risk stratification in early-stage EC. Also, the combination of ADC and D values demonstrated better diagnostic performance in identifying low-risk of early-stage EC compared to ADC or D values alone (0.904 vs. 0.892 vs. 0.823, respectively), which was similar to some other tumors [26,27]. Several previous studies have investigated the relationship between ADC values derived from single-b value DWI and the risk stratification of EC. Liu et al. [28] have retrospectively investigated the correlation of ADC values and the risk stratification of early-stage EC and have presented statistically significant difference between the low-risk and the intermediate/high-risk group ($0.851 \times 10^{-3} \text{ mm}^2/\text{s}$ vs. $0.725 \times 10^{-3} \text{ mm}^2/\text{s}$, $P = 0.0001$), which was consistent with our data.

However, Mainenti and his team [29] have demonstrated that the meanADC and minADC did not show any significant differences among the risk groups. This study included different tumor stages that were stratified into three classes of risk according to tumor grade and FIGO stage. The discordant reported results may be explained by the following: (1) the different risk stratification of EC: our study stratified the

⁹ESMO-ESGO-ESTRO: European Society for Medical Oncology-European Society of Gynaecological Oncology-European Society Therapeutic Radiation Oncology.

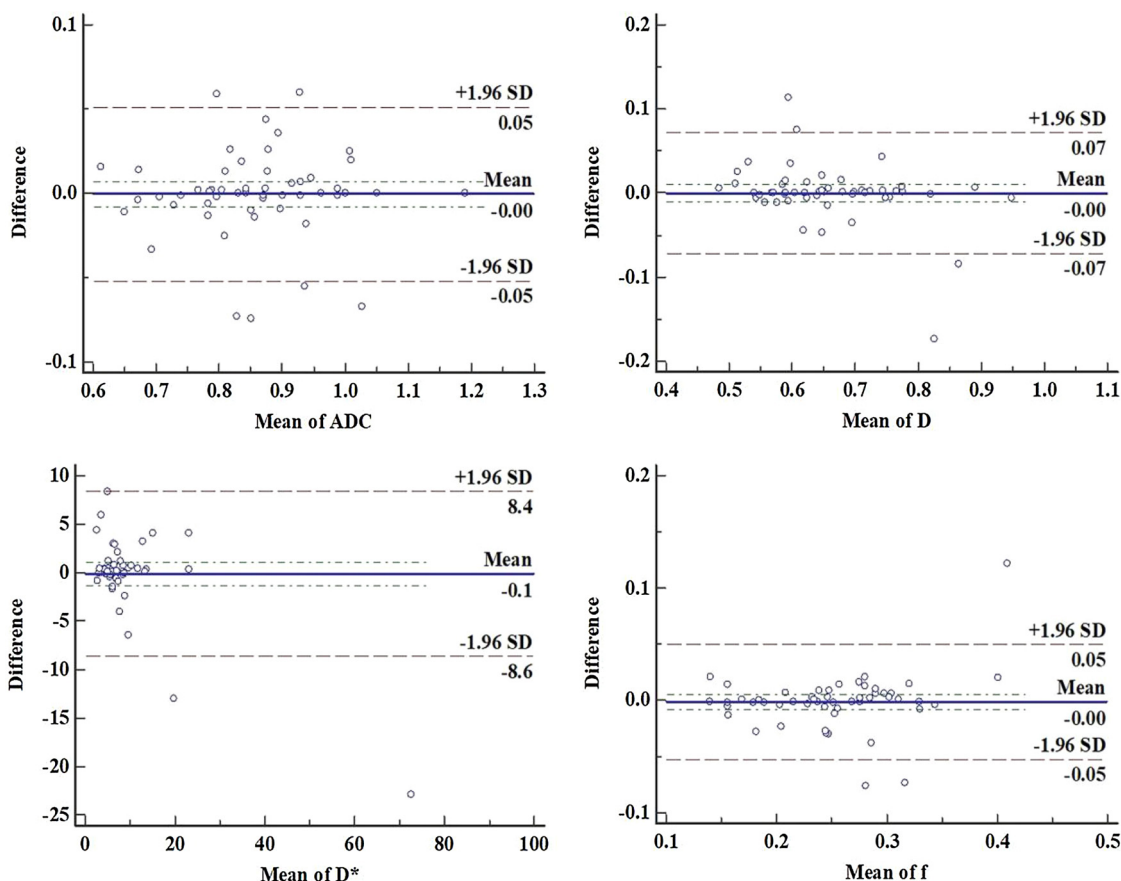


Fig. 2. By comparing the measurement of the two readers, Bland-Altman plots with 95% CI was used to evaluate the repeatability of the IVIM-derived parameters in EC. The mean difference of the two researchers measurements (y-axis) are plotted against the average of them (x-axis). The ADC, D, D* and f value showed excellent accordance of measurement by the two researchers.

three risk classes of early-stage EC according to the ESMO clinical practice guideline, while the previous study accorded to the tumor grade and FIGO stage to stratify the risk group (Low-risk group: stage IA with grade 1; Medium-risk group: stage IA with grade 3 or stage IB with any grade or stage II; High-risk group: stage III or IV); (2) insufficient number of patients enrolled in previous study (n = 28); (3) the variations of ROI positioning.

Moreover, in the present study, we also investigated the utility of perfusion parameters D* and f values and combined multi-b-value DWI derived parameters in differentiating low-risk group from non-low-risk group of early-stage EC. We found that D* values did not show any significant correlation with risk stratification of early-stage EC (r = 0.116, P = 0.407), while f values, an IVIM-derived perfusion parameters defined as the signal intensity ratio of blood capillaries and

Table 3
The multi-b-value parameters for risk stratification of early-stage EC.

Risk Stratification	ADC value ($\times 10^{-3} \text{ mm}^2/\text{s}$)	D value ($\times 10^{-3} \text{ mm}^2/\text{s}$)	D* value ($\times 10^{-3} \text{ mm}^2/\text{s}$)		f value
			M	Range	
Low-risk	0.900 ± 0.094	0.686 ± 0.094	6.210	2.260-61.100	0.267 ± 0.067
Intermedium-risk	0.749 ± 0.090	0.592 ± 0.076	6.405	3.010-11.900	0.200 ± 0.041
High-risk	0.746 ± 0.076	0.571 ± 0.040	10.100	6.930-17.100	0.239 ± 0.046
Low-risk VS. Intermedium-risk VS. high-risk					
P	0.000 ^a	0.001 ^a	0.088 ^b		0.013 ^a
F	15.205	7.755	4.850 ^c		4.467
Low-risk VS. Intermedium-risk					
P	0.000	0.011	-	-	0.011
Low-risk VS. High-risk					
P	0.001	0.013	-	-	0.914

ADC: apparent diffusion coefficient; AUC: area under the receiver operating characteristic curve; D: true diffusivity; D*: perfusion-related diffusivity; f: perfusion fraction; M: median.

^a The one-way analysis of variances (ANOVA).

^b Kruskal-Wallis test.

^c χ^2 .

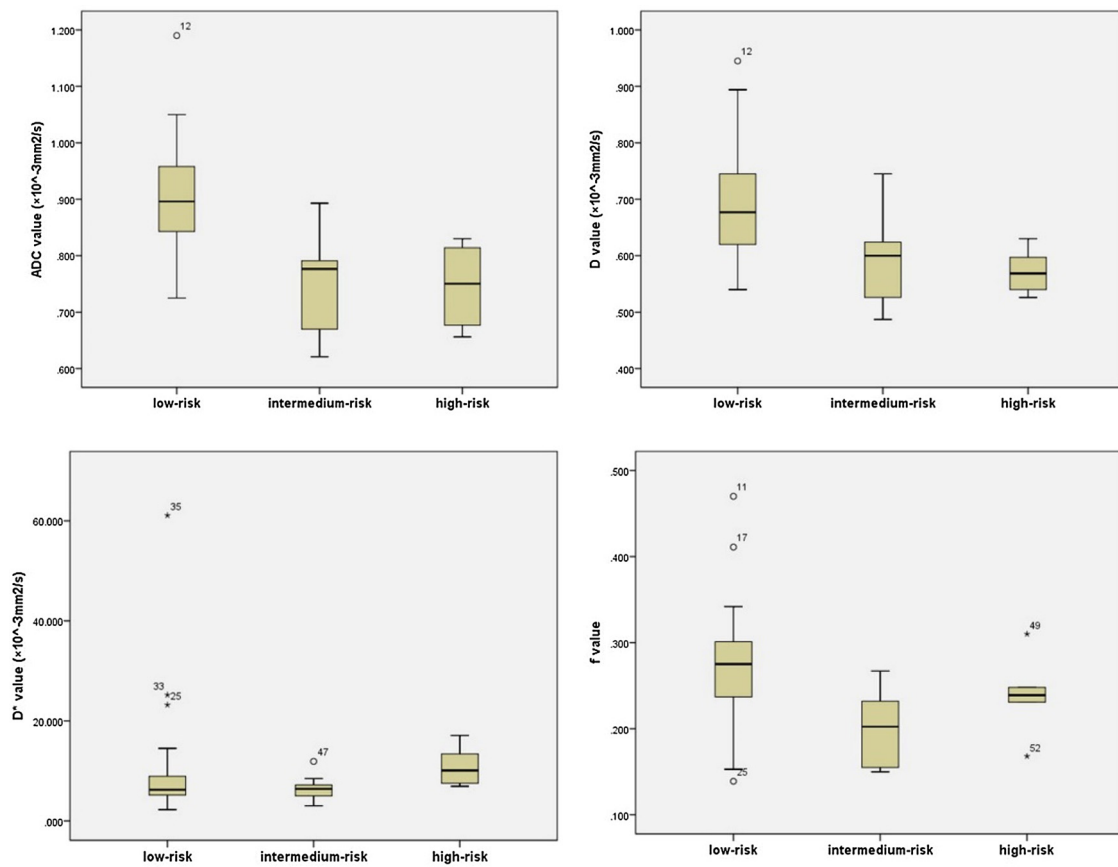


Fig. 3. Box-and-whisker plots show the ADC, D, D* and f values for the three risk stratification groups. Significant differences were found between the low-risk and intermedium-risk group for ADC, D and f values ($P < 0.05$). Significant differences were found in ADC and D values between the low-risk and high-risk group ($P < 0.05$); while no differences among the three risk stratification groups were observed for the D* value ($P = 0.088$).

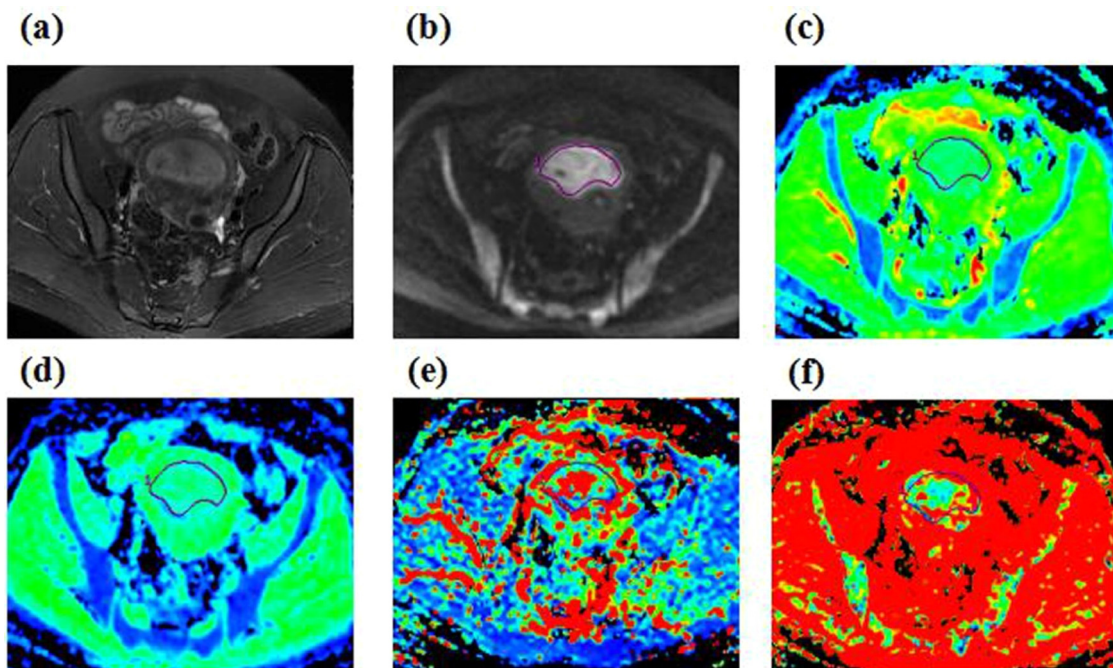


Fig. 4. (a) Axial T2-weighted image. (b-f) Multi-b-value DWI parametric maps. ADCmap (c), D map (d), D*map (e) and f map (f). Patient with low-risk endometrial carcinoma, FIGO IA, Grade 2. The ADC, D, D* and f value are $1.060 \times 10^{-3} \text{mm}^2/\text{s}$, $0.910 \times 10^{-3} \text{mm}^2/\text{s}$, $61.7 \times 10^{-3} \text{mm}^2/\text{s}$ and 0.193, respectively.

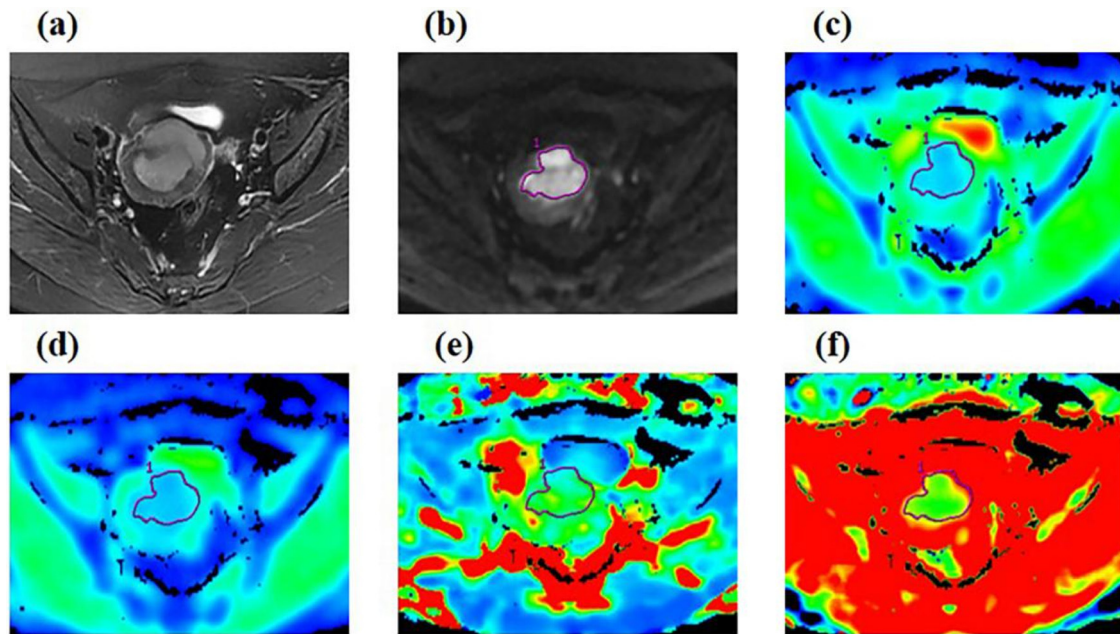


Fig. 5. (a) Axial T2-weighted image. (b-f) Multi-b-value DWI parametric maps. ADCmap (c), D map (d), D*map (e) and f map (f). Patient with high-risk endometrial carcinoma, FIGO IB, Grade 3. The ADC, D, D* and f value are $0.729 \times 10^{-3} \text{ mm}^2/\text{s}$, $0.547 \times 10^{-3} \text{ mm}^2/\text{s}$, $9.96 \times 10^{-3} \text{ mm}^2/\text{s}$ and 0.168, respectively.

Table 4

Diagnostic performance of ADC, D, f values and their combination parameters in identifying low-risk in early-stage EC.

Parameters	Optimal cut-off	AUC	Sensitivity (%)	Specificity (%)	Accuracy (%)
ADC ($\times 10^{-3} \text{ mm}^2/\text{s}$)	0.830	0.892	78.4%	87.5%	81.1%
D ($\times 10^{-3} \text{ mm}^2/\text{s}$)	0.630	0.823	73.0%	87.5%	77.4%
f	0.248	0.765	64.9%	87.5%	71.7%
ADC and f	0.701 ^a	0.912	81.1%	87.5%	83.0%
ADC and D	0.753 ^a	0.904	78.4%	87.5%	81.1%
D and f	0.650 ^a	0.894	83.8%	87.5%	84.9%

^a The optimal cut-off of combination is the optimal threshold of the predictive probability of combinations. ADC: apparent diffusion coefficient; AUC: area under the receiver operating characteristic curve; D: true diffusivity; D*: perfusion-related diffusivity; f: perfusion fraction.

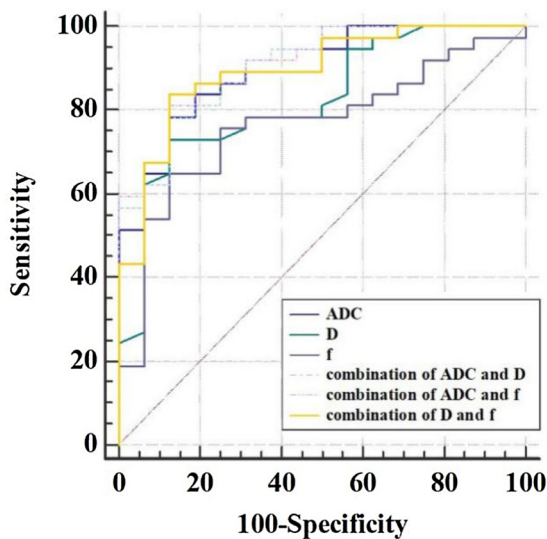


Fig. 6. Comparison of ROC curves for ADC, D, f values and the combination parameters in differentiating the low-risk and non-low-risk of early-stage EC. The combination of ADC and f values showed the highest AUC 0.912 for identification of low-risk of early-stage EC with the sensitivity of 81.1%, the specificity of 87.5% and the accuracy of 83.0%.

tumor tissues, showed significant difference between low-risk group and non-low-risk group and demonstrated the incremental value when combined with the other diffusion parameters. Especially, the combination of ADC and f values improved the AUC for the identification of low-risk of EC compared with the ADC or f values alone (0.912 vs. 0.892 vs. 0.765, respectively) with higher sensitivity (81.1% vs. 78.4% vs. 64.9%, respectively), which highlights the importance of multi-parametric MR imaging for the assessment of risk stratification at early-stage EC. Additionally, the combination of D and f values showed the highest sensitivity in distinguishing low-risk group from non-low-risk group compared with the combination of ADC and f values or the combination of ADC and D values (83.8% vs. 81.1% vs. 78.4%, respectively), which may provide another point of view to identify the low-risk of early-stage EC preoperatively. In general, studies investigating the value of quantitative parameters derived from novel MRI techniques for the risk stratification of early-stage EC are still lacking, and the current study exhibited promising results of single and combined multi-b-value DWI derived parameters for the assessment of risk stratification in early-stage EC.

The present study has some limitations. First, it was a single-center study with a relatively small sample size, especially regarding the type II EC due to its low incidence (10%–20%). Secondly, we did not perform the volumetric analysis in our study, which might be more representative of the intratumoral heterogeneity potentially reflecting tumor inherent aggressiveness. Nonetheless, this method was time-consuming and complicated, thus resulting in the increased measurement error and the decreased clinically practical value. Third, we performed

13 b values for multi-b-value DWI protocol, which prolonged the scan time and increased the probability of motion artefact. Further studies are needed to select and reduce the number of the optimal b values for multi-b-value DWI to make it more applicable and effective for the preoperative assessment of EC.

In conclusion, our study showed that multi-b-value DWI parameters were associated with the risk stratification of early-stage EC that could be conducive of the pre-treatment risk classification to facilitate the selection of the optimal therapeutic approach and meet the demand for greater personalization of cancer care.

Declaration of Competing Interest

We declare that we have no financial and personal relationships with other people or organizations that can inappropriately influence our work, there is no professional or other personal interest of any nature or kind in any product, service and/or company that could be construed as influencing the position presented in, or the review of, the manuscript entitled, "Multi-b-value Diffusion Weighted Imaging for Preoperative Evaluation of Risk Stratification in Early-stage Endometrial Cancer".

Acknowledgements

We gratefully acknowledge the assistance of Dr. Xie Lizhi, from GE Healthcare, MR Research China, Beijing, for support on IVIM methodology and writing assistance.

This research did not receive any specific grant from funding agencies in the public, commercial, or not-for-profit sectors

Appendix A. Supplementary data

Supplementary material related to this article can be found, in the online version, at doi:<https://doi.org/10.1016/j.ejrad.2019.08.006>.

References

- [1] R.L. Siegel, K.D. Miller, A. Jemal, *Cancer Statistics, 2017*, *CA Cancer J. Clin.* 67 (1) (2017) 7–30.
- [2] S. Bendifallah, G. Canlorbe, P. Collinet, et al., Just how accurate are the major risk stratification systems for early-stage endometrial cancer? *Br. J. Cancer* 112 (5) (2015) 793–801.
- [3] E.K. Nugent, E.A. Bishop, C.A. Mathews, et al., Do uterine risk factors or lymph node metastasis more significantly affect recurrence in patients with endometrioid adenocarcinoma? *Gynecol. Oncol.* 125 (1) (2012) 94–98.
- [4] A.N. Huijgens, H.J. Mertens, Factors predicting recurrent endometrial cancer, *Facts Views Vis. Obgyn* 5 (3) (2013) 179–186.
- [5] O. Gerner, A.B. Arie, T. Levy, et al., Lymphovascular space involvement compromises the survival of patients with stage I endometrial cancer: results of a multicenter study, *Eur. J. Surg. Oncol.* 33 (5) (2007) 644–647.
- [6] E. Sala, A. Rockall, R.A. Kubik-Huch, Advances in magnetic resonance imaging of endometrial cancer, *Eur. Radiol.* 21 (3) (2011) 468–473.
- [7] D.M. Larson, G.P. Connor, S.K. Broste, et al., Prognostic significance of gross myometrial invasion with endometrial cancer, *Obstet. Gynecol.* 88 (3) (1996) 394–398.
- [8] N. Colombo, E. Preti, F. Landoni, et al., Endometrial cancer: ESMO Clinical Practice Guidelines for diagnosis, treatment and follow-up, *Ann. Oncol.* 24 (Suppl. 6) (2013) i33–8.
- [9] M.Q. Bernardini, L.T. Gien, S. Lau, et al., Treatment related outcomes in high-risk endometrial carcinoma: canadian high risk endometrial cancer consortium (CHREC), *Gynecol. Oncol.* 141 (1) (2016) 148–154.
- [10] E. Sala, A.G. Rockall, S.J. Freeman, et al., The added role of MR imaging in treatment stratification of patients with gynecologic malignancies: what the radiologist needs to know, *Radiology* 266 (3) (2013) 717–740.
- [11] V. Vandecaveye, R. Dresen, F. De Keyser, Novel imaging techniques in gynaecological cancer, *Curr. Opin. Oncol.* 29 (5) (2017) 335–342.
- [12] A. Luomaranta, A. Leminen, M. Loukovaara, Magnetic resonance imaging in the assessment of high-risk features of endometrial carcinoma: a meta-analysis, *Int. J. Gynecol. Cancer* 25 (5) (2015) 837–842.
- [13] E. Epstein, L. Blomqvist, Imaging in endometrial cancer, *Best Pract. Res. Clin. Obstet. Gynaecol.* 28 (5) (2014) 721–739.
- [14] D. Le Bihan, Intravoxel incoherent motion perfusion MR imaging: a wake-up call, *Radiology* 249 (3) (2008) 748–752.
- [15] D. Le Bihan, E. Breton, D. Lallemand, et al., Separation of diffusion and perfusion in intravoxel incoherent motion MR imaging, *Radiology* 168 (2) (1988) 497–505.
- [16] V. Granata, R. Fusco, O. Catalano, et al., Intravoxel incoherent motion (IVIM) in diffusion-weighted imaging (DWI) for Hepatocellular carcinoma: correlation with histologic grade, *Oncotarget* 7 (48) (2016) 79357–79364.
- [17] N. Shen, L. Zhao, J. Jiang, et al., Intravoxel incoherent motion diffusion-weighted imaging analysis of diffusion and microperfusion in grading gliomas and comparison with arterial spin labeling for evaluation of tumor perfusion, *J. Magn. Reson. Imaging* 44 (3) (2016) 620–632.
- [18] H.B. Salvesen, I.S. Haldorsen, J. Trovik, Markers for individualised therapy in endometrial carcinoma, *Lancet Oncol.* 13 (8) (2012) e353–61.
- [19] W.J. Koh, N.R. Abu-Rustum, S. Bean, et al., Uterine neoplasms, version 1.2018, NCCN clinical practice guidelines in oncology, *J. Compr. Cancer Netw.* 16 (2) (2018) 170–199.
- [20] S. Bendifallah, E. Darai, M. Ballester, Predictive modeling: a new paradigm for managing endometrial cancer, *Ann. Surg. Oncol.* 23 (3) (2016) 975–988.
- [21] H.S. Kim, D.H. Suh, M.K. Kim, et al., Systematic lymphadenectomy for survival in patients with endometrial cancer: a meta-analysis, *Jpn. J. Clin. Oncol.* 42 (5) (2012) 405–412.
- [22] H. Kitchener, A.M. Swart, Q. Qian, et al., Efficacy of systematic pelvic lymphadenectomy in endometrial cancer (MRC ASTEC trial): a randomised study, *Lancet* 373 (9658) (2009) 125–136.
- [23] N. Colombo, C. Creutzberg, F. Amant, et al., ESMO-ESGO-ESTRO consensus conference on endometrial cancer: diagnosis, treatment and follow-up, *Int. J. Gynecol. Cancer* 26 (1) (2016) 2–30.
- [24] K. Kishimoto, S. Tajima, I. Maeda, et al., Endometrial cancer: correlation of apparent diffusion coefficient (ADC) with tumor cellularity and tumor grade, *Acta Radiol.* 57 (8) (2016) 1021–1028.
- [25] J.X. Jiang, J.L. Zhao, Q. Zhang, et al., Endometrial carcinoma: diffusion-weighted imaging diagnostic accuracy and correlation with Ki-67 expression, *Clin. Radiol.* 73 (4) (2018) 411–413.
- [26] C. Liu, C. Liang, Z. Liu, et al., Intravoxel incoherent motion (IVIM) in evaluation of breast lesions: comparison with conventional DWI, *Eur. J. Radiol.* 82 (12) (2013) e782–9.
- [27] C. Ma, Y. Li, L. Wang, et al., Intravoxel incoherent motion DWI of the pancreatic adenocarcinomas: monoexponential and biexponential apparent diffusion parameters and histopathological correlations, *Cancer Imaging* 17 (1) (2017) 12.
- [28] J. Liu, F. Yuan, S. Wang, et al., The ability of ADC measurements in the assessment of patients with stage I endometrial carcinoma based on three risk categories, *Acta Radiol.* (2018) 17693673.
- [29] P.P. Mainenti, L.M. Pizzuti, S. Segreto, et al., Diffusion volume (DV) measurement in endometrial and cervical cancer: a new MRI parameter in the evaluation of the tumor grading and the risk classification, *Eur. J. Radiol.* 85 (1) (2016) 113–124.